RESILIENT INFRASTRUCTURE

June 1 - 4, 2016

AERODYNAMIC OPTIMIZATION TO REDUCE WIND LOADS ON TALL BUILDINGS

Ahmed Elshaer
WindEEE Research Institute, Western University, Canada

Girma Bitsuamlak
WindEEE Research Institute, Western University, Canada

Ashraf El Damatty
WindEEE Research Institute, Western University, Canada

ABSTRACT

Wind is one of the governing load cases for tall building design, which produces high level of straining actions, deflections and lateral and transverse vibrations. Keeping those vibrations within the comfort limits is becoming a key aspect in tall building design, especially for buildings with high aspect ratio. Improving the aerodynamic performance of the tall building by modifying its shape can lower building motions, which reduces the additional expenses for external damping systems and alleviate the high cost associated with lateral support systems. In the present study, an aerodynamic shape optimization procedure is developed by combining Computational Fluid Dynamics (CFD), optimization algorithm and Artificial Neural Network (ANN). The developed procedure utilizes ANN as a surrogate model for evaluating aerodynamic properties, which is pre-trained using two-dimensional CFD analysis. The current study investigates the validity of the developed procedure by conducting a high accuracy, three-dimensional Large Eddy Simulation (LES) based analysis on the optimal building shapes. It was observed that utilizing two-dimensional CFD simulations in the optimization procedure can help identify effective cross-sections of tall buildings.

Keywords: Wind load; CFD; Tall Building; Wind Response; Large Eddy Simulation (LES); Complex surrounding

1. INTRODUCTION

Enhancing resiliency and sustainability of buildings requires a climate responsive design procedure. For example, wind is the governing design load case for typical tall buildings. Huge amount of resources is drawn to control loads and vibrations caused by wind (Kareem et al. 1999). A large portion of those expenses and materials can be saved by improving the aerodynamic performance of tall buildings. This improvement can be reached by modifying the outer shape of tall buildings locally at the corners or globally over the height and the width of the building (Kwok et al. 1988, Tamura and Miyagi 1999, Carassale et al. 2014, Elshaer et al. 2014); the common method for studying aerodynamic mitigations of buildings is conducting BLWT tests. This approach is useful to compare different feasible shapes of tall buildings. However, a wide part of the search space remains unexplored as the search space is only limited to the tested options (Bernardini et al. 2015). In addition, utilizing BLWT tests are considered costly and time-consuming tool for investigating a wide range of the possible options. On the other hand, CFD can explore more alternatives to reach the optimal shape, which is increasing the interest in that subject (Bobby et al. 2013). Thus, the aerodynamics shape optimization research is primarily adopting CFD because of its applicability to be integrated with optimization algorithms. Kareem et al. (2013a, b and 2014) introduced an innovative tool for tall building shape optimization by adopting low-dimensional steady CFD models. This approach is capable of overcoming the computational challenge associated with the iterative procedure required for optimization.

In the current study, a new hybrid optimization framework is developed by coupling optimization algorithm, CFD solver and Artificial Neural Network (ANN) model. The optimization algorithm is used to search for the optimal building shape by altering the geometric parameters controlling the building shape. The unsteady CFD analyses are

conducted for selected samples to train the ANN with a database of shapes and corresponding aerodynamic properties. The computationally less expensive, ANN model, is then utilized as a surrogate model to estimate the aerodynamic properties during the optimization procedure. Using ANN in the optimization procedure eliminates the need for sequential iterative computationally demanding CFD analyses, which significantly reduces the required execution time (i.e. around 250 times faster than sequential procedure). Finally, a verification stage is conducted by comparing the optimal solution to less optimal shapes obtained during the optimization procedure. Consistent Discrete Random Flow Generator (CDRFG) technique (Aboshosha et al. 2015) is utilized for synthesizing the inflow. Two illustration examples are presented to demonstrate the capability of the proposed framework.

2. HYBRID AERODYNAMIC OPTIMIZATION FRAMEWORK

The Hybrid Aerodynamic Optimization (HAO) procedure begins by defining the objective function, which is the aerodynamic property aimed to be minimized or maximized, such as drag and/or lift. The value of the objective function for each shape depends on the building geometry, which is controlled by the optimization design variables. Then, the optimization algorithm is used to find the optimal combination of design variables that produces the highest fitness to the objective function. The current study adopts the Genetic Algorithm (GA). GA requires multiple evaluations for the objective functions during the iterative procedure of the optimization. The evaluation of the objective function is conducted using the ANN model that had been previously trained using 2D-CFD simulations. After predicting the optimal building shape, a verification step is carried out by comparing the optimal solution to lower fitness shapes using high accuracy 3D-CFD simulations. Figure 1 summarizes the framework of the proposed hybrid aerodynamic optimization procedure.
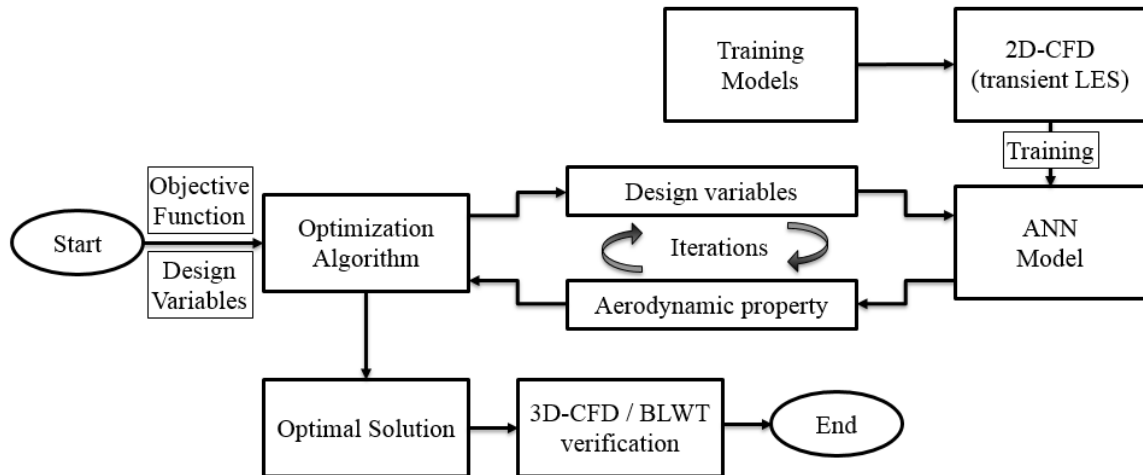

Figure 1: Hybrid Aerodynamic Optimization framework

The optimization technique used in the current study is the GA, where design variables are coded as real numbers. The major advantage of this technique over the gradient-based classical techniques is its capability of locating the global extreme value (i.e. maximum or minimum) without being trapped in a local extreme value. This key capability results from starting the search process from multiple points in the search space, instead of moving from a single point like gradient-based methods. GA is found to be efficient in estimating the optimal solution in similar complex optimization problems such as Zhou and Haghighat (2009) and El Ansary et al. (2011). A complete description of GA technique is given by Goldberg (1989) and Davis (1991). The summary of the optimization procedure using GA is presented in Figure 2.
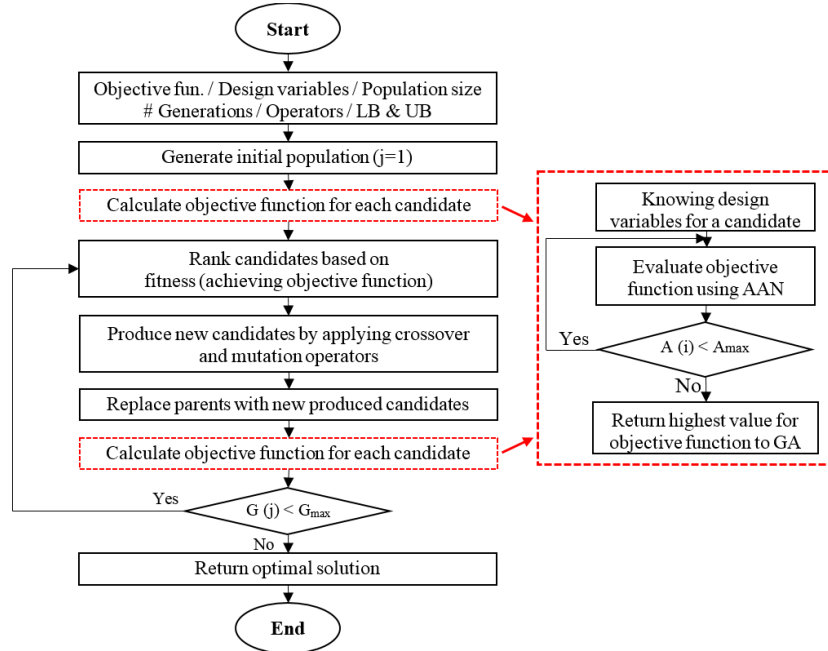
Figure 2: Genetic Algorithm flowchart

Using GA as an optimization technique requires numerous evaluations for the objective function due to having multiple initial candidates and many generations. These evaluations become more challenging when the objective function is computationally expensive such as CFD analyses. Therefore, a surrogate model can be used for estimating the objective function after being trained using a database of building samples and their corresponding objective function values resulting from CFD simulations. The utilization of a surrogate model in the optimization procedure will (1) significantly reduces the computational cost, (2) eliminates the need for direct integration of CFD solver within the optimization procedure and (3) facilitates the use of any available experimental BLWT results in conjunction with the CFD database. In the current study ANN model is adopted as a surrogate model for objective function evaluation. This numerical model is commonly used to estimate output values depending on input values after being trained by a database of inputs and outputs. Thus, in an optimization problem, a well-trained ANN model will result in a reliable estimate for objective function. The utilization of ANN as an alternative for objective function evaluation was also reported in other optimization problems such as natural ventilation (Zhou and Haghighat, 2009). ANN was previously adopted by the authors in optimizing a building shape for reducing wind drag (Elshaer et al. 2015a) and controlling the building vibrations due to wind (Elshaer et al. 2015b).

3. ILLUSTRATION OPTIMIZATION PROBLEMS

In the current study, two optimization problems are conducted to examine the efficiency of the proposed optimization framework. Problem 1 aims to find the optimal tall building cross-section that reduces the wind drag forces, while Problem 2 targets to find the optimal cross-section reducing the wind lateral vibration. Thus, the objective functions are set to be the mean drag coefficient ($\overline{C_D}$) and the standard deviation of the lift coefficient (C_L') in problem 1 and 2, respectively. For each combination of design variables (candidate), the objective function is defined to be the critical wind direction. The C_D and C_L are evaluated using Eq. [1]. The basic building cross-section is chosen to be a square of 50 mm side length similar to previous wind tunnel studies from the literature (Tamura et al. 1998, Kawai 1998, Tamura and Miyagi 1999). The design variables (v_1 and v_2) are defined to control the corner shape following Eq. [2]. Figure 3 shows the geometry parameters of the tall building cross-section. In order to the building shape in an accepted architectural shape, lower bound (LB) and upper bound (UB) are set for each design variable. For v_1, LB and UB are set to be 0.01 and 0.2, respectively. While for v_2, they are set to be -1.0 and 2.0.

$$[1] \quad C_D = \frac{F_D}{\frac{1}{2}\rho v_{ref}^2 A_p}, \quad C_L = \frac{F_L}{\frac{1}{2}\rho v_{ref}^2 A_p}$$

where F_D and F_L are the along- and across- wind forces, respectively, ρ is the air density, v_{ref} is the reference velocity at the building height and A_p is the building projected cross-section area.

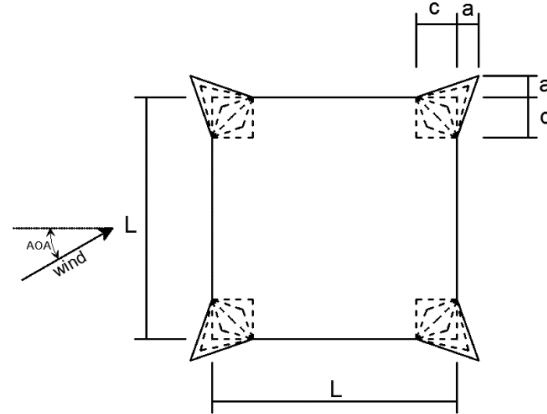$$[2] \quad v_1 = \frac{c}{L}, \quad v_2 = \frac{a}{c}$$

Figure 3: Geometric parameters of the study section

In order to train the ANN, CFD analyses are required for training samples to build a database of design variables, wind angle of attack (AOA) and the corresponding objective function values. The training samples are selected to be random combinations of design variables and AOA to capture the variability of the ANN outputs (objective function values) with the inputs (design variables and AOA), as shown in Figure 4. After selecting the required training samples, an initial graphics exchange specification (iges) file is generated for each input sample using AutoLisp (AutoCAD) to be readable for the CFD solver. (STAR-CCM+ v.10.06) package is utilized to solve the CFD analyses using the SharcNet high performance computer facility at the University of Western Ontario. Time history data for C_D and C_L are extracted from executed models to evaluate $\overline{C_D}$ and $C_L{}'$. A MATLAB code is utilized to automate the procedure of selecting samples, generating (iges) files, building CFD models, submitting jobs for SharcNet and extracting the output from CFD models.
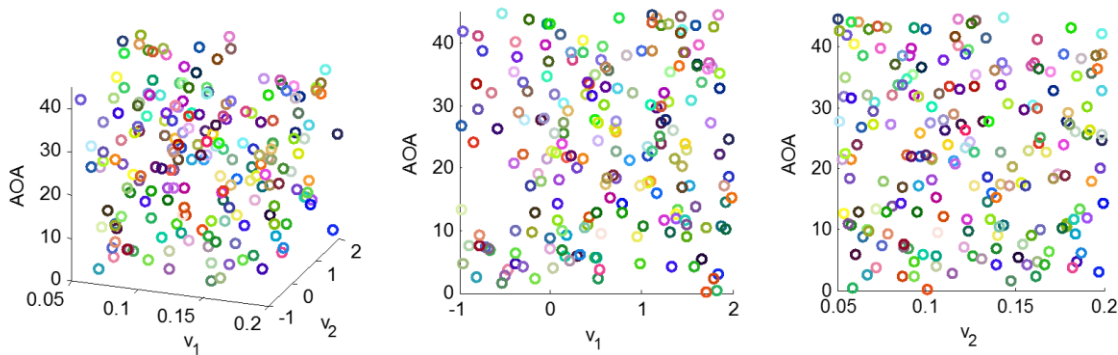

Figure 4: Training samples for Artificial Neural Network model

Two-dimensional Large eddy simulation (LES) is conducted for each sample using a length scale of 1:500, time scale of 1:100, and a uniform inlet velocity of 10 m/s. The outlet is considered to be a pressure outlet. Top, bottom and the two sides are assigned a symmetric plane. All the building faces are assigned as "No-slip" walls. The total number of mesh cells in each model was more than 200,000 cells. The polyhedral mesh size was less than ($L/20$), where L is the width of the building. The dimensions of the employed computational domain follow the recommendation of COST 2007 guidelines Franke et al. 2007. The dynamic Sub-Grid Scale model by Smagornisky (1963) and Germano et al. (1991) is used to account for the turbulence. In order to ensure the convergence and the accuracy of the solution, Courant Friedrichs-Lewy (CFL) is maintained less than 1.0 by setting the sol time step to be 0.0005 sec (i.e. maximum CFL ~ 0.5 at the top of the building). Each simulation is resolved to 1000 time steps representing 0.5 second in model-scale (i.e. 0.8 minute in full-scale).

A database of 200 samples is utilized to train the ANN model for evaluating the objective function. This database is formed of different combinations of v_1, v_2, AOA and the corresponding objective function values obtained from the CFD analyses. 70% of the samples are used to train the ANN, while 30% are used to validate and test the developed model. Figure 5 shows the error distribution and the regression plot of the ANN model. The error in objective function evaluation using ANN model doesn't exceed 5% in 60% of the utilized database. The regression coefficient between the developed model and the fitting database is found to be 0.979. These accuracy parameters reflect the capability of ANN as a fitting tool.
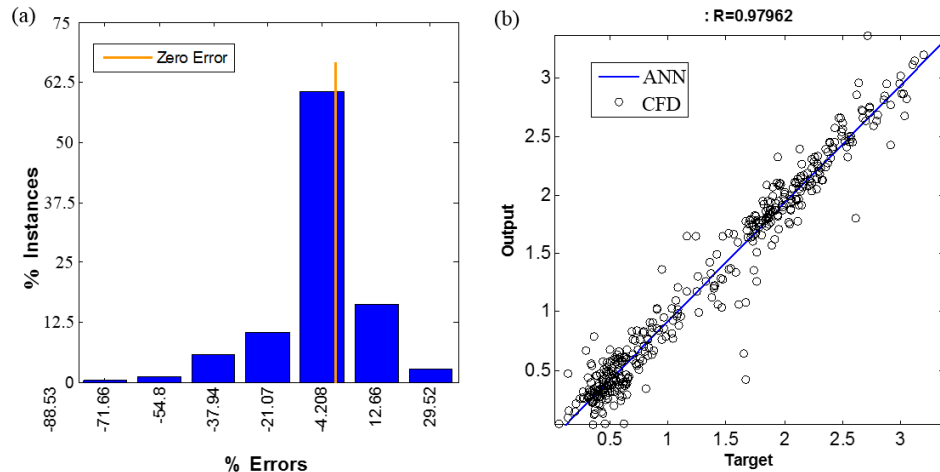

Figure 5: (a) Error distribution and (b) regression plot for the ANN model

4. RESULTS AND VERIFICATION OF THE OPTIMIZATION PROBLEMS

The optimization procedure is conducted for the two optimization problems until the optimal solutions are obtained after 40 generations. Figure 6 shows the fitness curves for the optimization problems where the objective function value of the best fitness candidate in each generation is plotted versus the generation number. This figure illustrates the improvement of the aerodynamic properties (objective functions) over optimization generations. For optimization problem 1, the mean drag coefficient ($\overline{C_D}$) of the optimal cross-section is 1.335, which is 30% lower than that of sharp edge square. While for problem the standard deviation of the lift coefficient (C_L') of the optimal solution is 0.503. The optimal solution lowered the C_L' by 24% than that of sharp edge square.
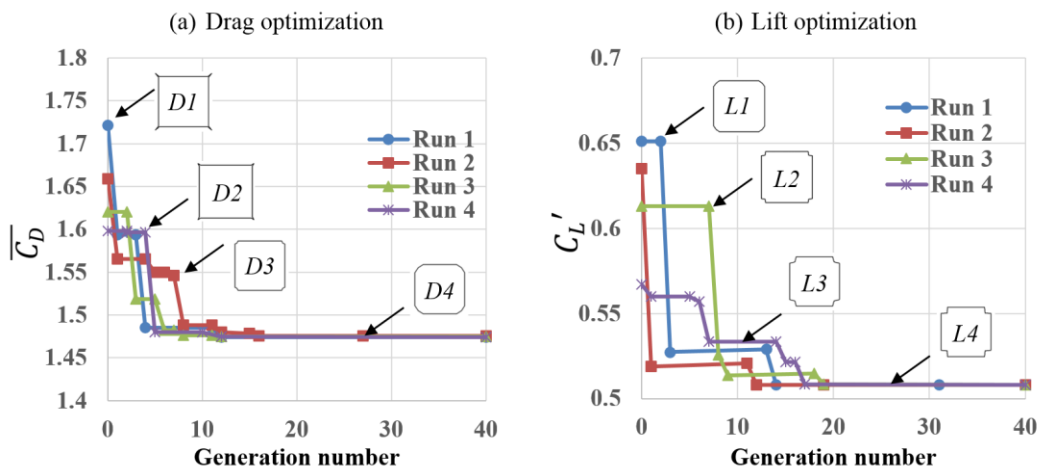

Figure 6: Fitness curves for the (a) drag and (b) lift optimization problems

So as to verify the obtained optimal solution, additional three cross-sections of lower fitness are selected from the fitness curve in each optimization problem to be compared to the optimal solution. Figure 7 shows the design variables

of the selected cross-sections as well as the optimal cross-section for drag and lift optimization problems. These cross-sections are investigated using three-dimensional CFD simulations to verify the aerodynamic improvement resulted from the optimization procedure. Figure 7 also shows the surface plots of the objective functions evaluated using the ANN model. It can be noticed that the optimization algorithm is able to locate the global optimal solution without being trapped in a local minimum. It is noticed that the ANN model is found to be capable of fitting objective functions of complex shape, which indicates the efficiency of ANN as a surrogate model for objective function evaluation
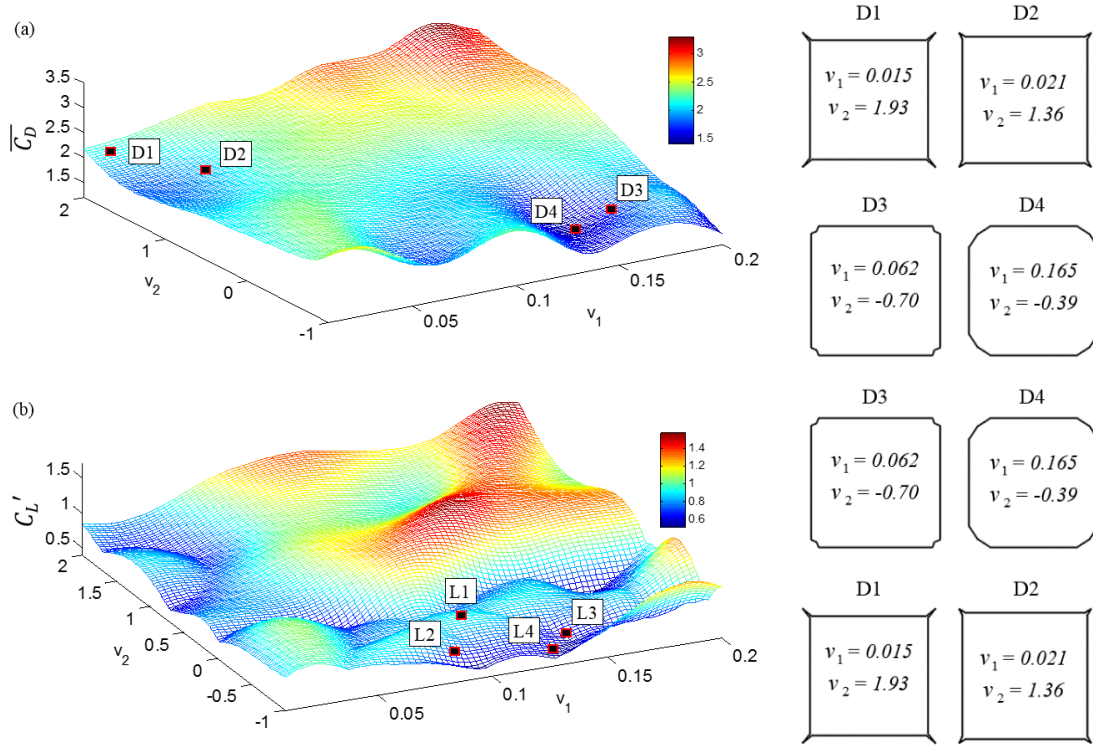

Figure 7: Selected cross-sections from (a) drag and (b) lift optimization problems; surface plot for the ANN model of the (c) mean drag and (d) fluctuating lift coefficients

Three-dimensional LES are conducted for the optimal and the selected cross-sections to verify the accuracy of low-dimensional models and ANN in HAO procedure. The used length and time scales are 1:400 and 1:100, respectively, with a mean wind velocity of 10 *m/s* at the building height. Computational domain dimensions are chosen based on the recommendation of COST (2007), Frank (2006) and Dagnew and Bitsuamlak (2013). CDRFG technique is utilized to generate a turbulent inflow because of its proven accuracy for isolated (Aboshosha et al. 2015) and complexly surrounded (Elshaer et al. 2016) tall buildings. The generated wind velocity and turbulence profiles are following ESDU 2011 assuming open terrain exposure. Figure **8** shows the velocity, the turbulence intensity and the turbulence length scale profiles used for generating the inflow fields using CDRFG technique. The sides and the top of the computational domain are assigned as a symmetry plane boundary condition, while the bottom of the computational domain and all building faces are defined as no-slip walls. Figure 9 shows the computational domain dimensions and the boundary conditions for the LES.

Polyhedral control volumes are used to discretize the computational domain. The utilized grid sizes are divided into three zones based on the flow structures that required to be captured. Zone 1 is located away from the building of interest where the grid size is maximum. Zone 3 is located close to the building of interest where finer grid size is utilized to capture important flow details of in the wake zone and the zone around the study building. Zone 2 is located between zone 1 and 3 where intermediate grid size is used. The employed grid zones and sizes are selected similar to those adopted by the authors in Elshaer et al. (2016). A number of 15 prism layers parallel to the study building surfaces with a stretching factor of 1.05 is utilized in zone 3 satisfying the recommendations by Murakami, COST and Tominaga et al. Figure 9shows the utilized grid in the LES for the current study.

The simulations are conducted using a commercial CFD package (STAR-CCM+ v.10.06) employing LES with dynamic sub-grid scale model by Smagornisky (1963) and Germano et al. (1991). Each simulation is resolved for 4,000 time steps representing 2 seconds in model-scale (i.e. 3.5 minutes in full-scale). SharcNet high performance computer (HPC) facility at the Western University is utilized for conducting the numerical simulations. The computational time required for each simulation is 3 hours on 128 processors.
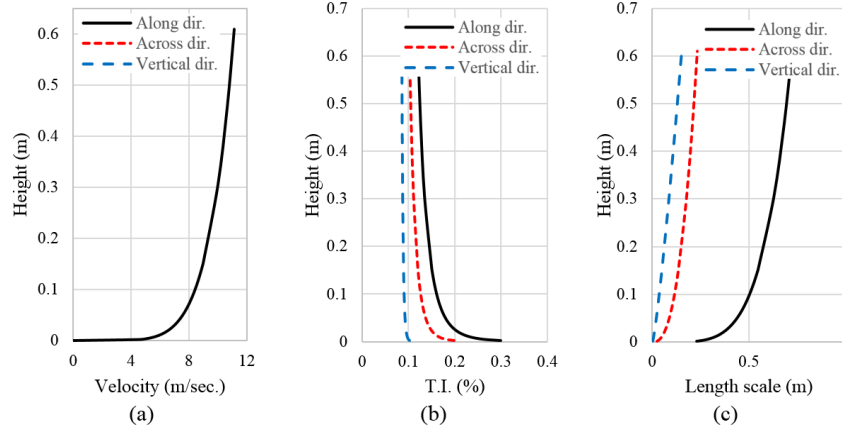

Figure 8: (a) velocity, (b) turbulence intensity and (c) turbulence length scale profiles used for inflow generation using CDRFG technique
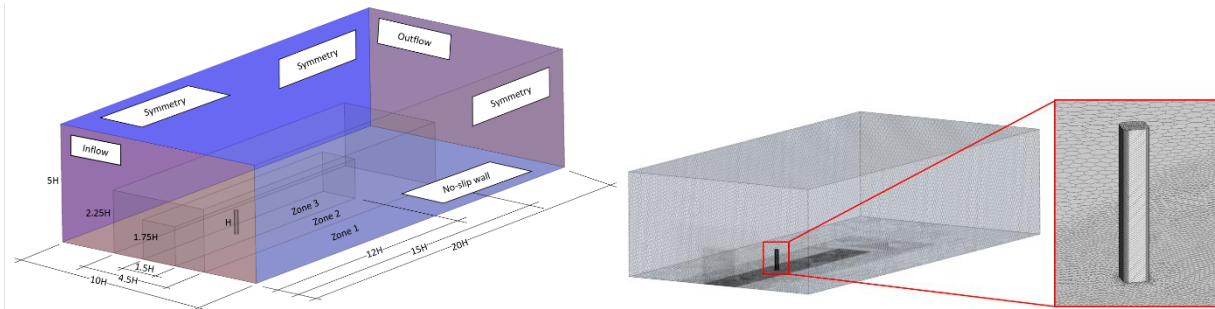

Figure 9: Computational domain dimensions and boundary conditions and Grid resolution utilized for the 3D-CFD simulations

So as to compute the building responses for different cross-section shapes, the time histories of the base moments are extracted from the LES. Figure 10a shows the time histories of the normalized along-wind moment for the cross-sections from the drag optimization problem, while Figure 10b shows the time histories of the normalized across-wind moment for the cross-sections from lift optimization problem. The base moments are normalized using **Error! Reference source not found.**. It can be noticed that the along-wind moment is decreasing for higher drag fitness cross-sections, while the fluctuation in the across-wind moments decreases for higher lift fitness cross-sections.

$$[3] \quad M_{yref} = \frac{1}{2}\rho V_h^2 B_y H^2 \quad , M_{xref} = \frac{1}{2}\rho V_h^2 D_x H^2, \quad M_{zref} = \frac{1}{2}\rho V_h^2 D_x B_y H$$

where V_h is the mean velocity at the building height, ρ is the air density which is taken equal to 1.25 kg/m^3, B_y is the building width (normal to wind direction) and D_x is the building depth (along wind direction)
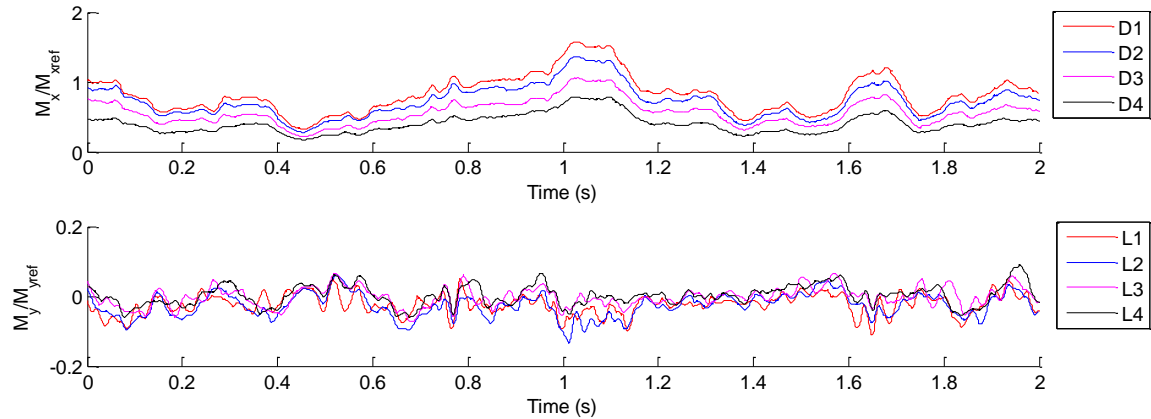
Figure 10: Base moment time histories around (a) x-axis (along-wind) of cross-sections from drag optimization and (b) around y-axis (across-wind) of cross-sections from lift optimization

Figure 11 shows the smoothed Power Spectral Density (PSD) plots, which illustrates the energy distribution corresponding to each frequency. The PSD plots are computed for the optimal shapes and the other selected cross-sections from both optimization problems. As shown in this figure, the aerodynamic improvement can be observed for the optimal solutions compared to the less fitness sections. For the lift optimization problem, it is also noticed that, the optimal section (L4) has a broader peak than the other cross-sections, which reflects the reduction in the energy associated with the vortex shedding frequency.
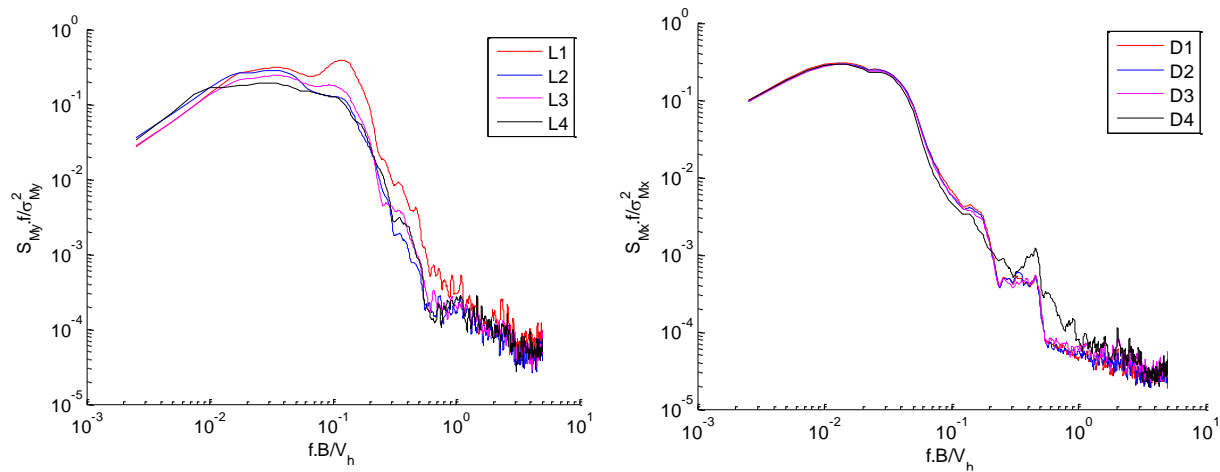

Figure 11: Base moments spectra (a) around x-axis (along-wind) of cross-sections from drag optimization and (b) around y-axis (across-wind) of cross-sections from lift optimization

PSD are used to evaluate the dynamic responses for different cross-sections using the method described by Kareem and Kijewski 1999 and Kareem and Chen 2005. For the drag optimization cross-sections, the peak top displacement, acceleration and the base moment are plotted in Figure 12a in the along-wind direction. The optimal cross-sections (D4) shows lower values of dynamic responses than other less optimal cross-sections by 29%. Similarly, for the lift optimization, Figure 12b plots the peak top displacement, acceleration and the base moment in the across-wind direction. The figure indicates up to 52% reduction in the dynamic responses of the optimal cross-section (L4) compared to less optimal cross-sections. This reduction in motion and forces will result in significant reduction in the required building materials, damping systems and consequently cost.
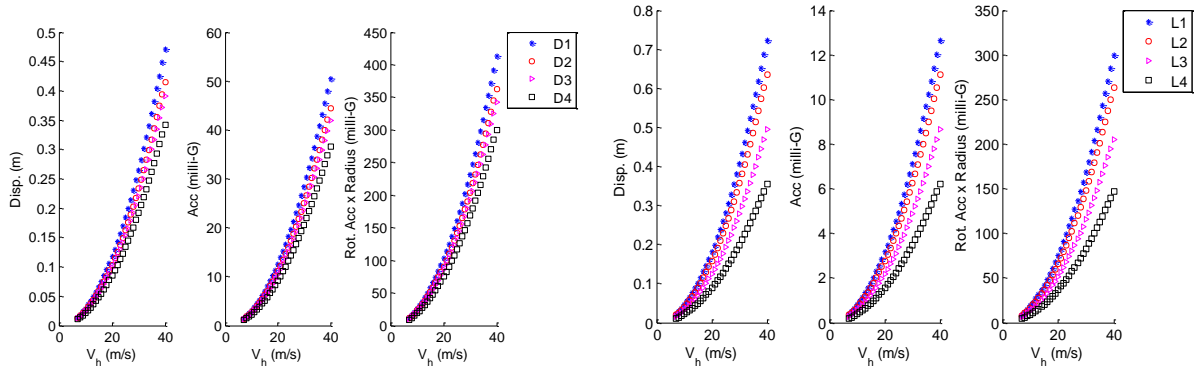
Figure 12: (a) Peak top floor displacement, (b) acceleration, (c) base moments in the along-wind direction of cross-sections from drag optimization; (d) Peak top floor displacement, (e) acceleration and (f) base moments in the across-wind direction of cross-sections from lift optimization

5. CONCLUSIONS

The current study introduces a robust optimization procedure called the Hybrid Aerodynamic Optimization (HAO), which combines the Genetic Algorithm (GA), the Computational Fluid Dynamics (CFD) solver and the Artificial Neural Networks (ANN) model. During the optimization procedure, ANN model is utilized as a surrogate model for objective function evaluation after being trained by a database of aerodynamic properties resulted from two-dimensional CFD (2D-CFD) analyses. Two optimization problems are demonstrated to examine the proposed HAO procedure in optimizing drag and lift by modifying the corner shapes of a tall building. A verification stage is conducted to ensure the capability of HAO procedure by conducting three-dimensional CFD (3D-CFD) analyses to the optimal shapes resulted from HAO procedure. Based on the proposed aerodynamic optimization procedure and presented examples, the following conclusions are deduced:

- Using ANN as an alternative to the expensive CFD analyses in HAO (1) eliminates the need for direct integration of CFD solver within the optimization procedure (2) facilitates the use of any available experimental BLWT results in conjunction with the CFD database and (3) accelerates the computational time required for the optimization process.
- ANN model is capable of capturing complex variations in the objective function, which results in better fitting to the training data (i.e. regression coefficient = 0.979).
- The two-dimensional LES model provides satisfactory accuracy for comparing local (corner) modifications in addition to significant reducing in the required computational time.
- Despite the multiple extreme values in the objective function, Genetic Algorithm (GA) is capable of estimating the global optimal solution without being trapped in a local extreme value.
- For the drag optimization problem, the mean drag coefficient ($\overline{C_D}$) is lower by 30% for the optimal shape compared to the sharp edge corner. While in the lift optimization problem the standard deviation of the lift coefficient ($C_L{'}$) is reduced by 24% for the optimal corner compared to the sharp edge one.

REFERENCES

Aboshosha, H., Elshaer, A., Bitsuamlak, G., El Damatty, A., 2015a. Consistent inflow turbulence generator for LES evaluation of wind-induced responses for tall buildings. Journal of Wind Engineering and Industrial Aerodynamics. 142, 198-216.

Ansary, A., El Damatty A., Nassef, A., 2011. Optimum Shape and Design of Cooling Towers. World Academy of Science. Engineering and Technology 9, 4-13.

Bernardini, E., Spence, S., Wei, D., Kareem A., 2015. Aerodynamic shape optimization of civil structures: A CFD-enabled Kriging-based approach. Journal of Wind Engineering and Industrial Aerodynamics 144, 154-164.

Bobby, S., Spence, S., Bernardini, E., Wei, D., Kareem, A., 2013. A Complete Performance-based Optimization Framework for the Design of Tall Buildings. Proceeding of 11th International conference on Structural Safety and Reliability, New York, US.

Carassale, L., Freda, A., Marrè-Brunenghi M., 2014. Experimental investigation on the aerodynamic behavior of square cylinders with rounded corners. Journal of Fluids and Structures 44, 195-204.

Chen X, Kareem A., 2005. Dynamic wind effects on buildings with 3-D coupled modes: application of HFFB measurements. Journal of Engineering Mechanics; ASCE, 131(11), 1115-1125.

Davis L., 1991. Handbook of Genetic Algorithms, Van Nostrand Reinhold, New York.

Elshaer, A., Bitsuamlak, G., El Damatty, A., 2014. Wind Load Reductions due to Building Corner Modifications. 22nd Annual Conference of the CFD Society of Canada. Toronto, Canada.

Elshaer, A., Bitsuamlak, G., El Damatty, A., 2015a. Aerodynamic shape optimization for corners of tall buildings using CFD. 14th International Conference on Wind Engineering. Porto Alegre, Brazil.

Elshaer, A., Bitsuamlak, G., El Damatty, A., 2015b. Vibration control of tall buildings using aerodynamic optimization. 25th Canadian Congress of Applied Mechanics, London, Canada.

Franke J., 2006. Recommendations of the COST action C14 on the use of CFD in predicting pedestrian wind environment. The forth international Symposium on Computational Wind engineering; Yokohama, Japan. 529-523.

Germano, M., Piomelli, U., Moin, P., Cabot, W., 1991. A dynamic subgrid-scale eddy viscosity model. Physics of Fluids 3(7), 1760-1765.

Goldberg D., 1989. Genetic Algorithms in search. Optimization and Machine Learning. Addison-Wesley Publishing Company, Inc., New York.

Kareem, A., Bernardini, E., Spence, S.M.J., 2013a. Control of the Wind Induced Response of Structures. Springer, Tokyo, Japan, pp. 377–410 (Chapter14).

Kareem, A., Bobby, S., Spence, S.M.J., Bernardini, E., 2014. Optimizing the form of tall buildings to urban environments. In: CTBUH 2014 International Conference.

Kareem, A., Kijewski, T., & Tamura, Y. 1999. Mitigation of motions of tall buildings with specific examples of recent applications. Wind and structures 2(3), 201-251.

Kareem, A., Spence, S.M.J., Bernardini, E., Bobby, S., Wei, D., 2013b. Using computational fluid dynamics to optimize tall building design. CTBUHJ. (III), 38-42.

Kawai, H., 1998. Effects of corner modifications on aeroelastic instabilities of tall buildings. Journal of Wind Engineering and Industrial Aerodynamics 74-76, 719-29.

Kwok, KCS., 1988. Effects of building shape on wind-induced response of tall buildings. Journal of Wind Engineering and Industrial Aerodynamics 28, 381-90.

SHARCNET 2016: a consortium of colleges, universities and research institutes operating a network of high-performance computer clusters across south western, central and northern Ontario. [Online]. Available: www.sharcnet.ca.

Smagorinsky J., 1963. General circulation experiments with the primitive equations. I. the basic experiment. Monthly Weather Review 91, 99-164.

STAR CCM+, 2016. v.10.06, CD-ADAPCO Product, www.cd-adapco.com/products.

Tamura, T., Miyagi, T., 1999. The effect of turbulence on aerodynamic forces on a square cylinder with various corner shapes. Journal of Wind Engineering and Industrial Aerodynamics 83, 135-145.

Tamura, T., Miyagi, T., Kitagishi, T., 1998. Numerical prediction of unsteady pressures on a square cylinder with various corner shapes. Journal of Wind Engineering and Industrial Aerodynamics 74–76, 531-542.

Zhou, L., Haghighat, F., 2009. Optimization of ventilation system design and operation in office environment, Part I: Methodology. Building and Environment 44(4).